Surface structure of $Au_3Cu(001)$

G. A. Eckstein,* S. Maupai, A. S. Dakkouri, and M. Stratmann
Lehrstuhl für Korrosion und Oberflächentechnik (LKO), Universität Erlangen-Nürnberg, Martensstrasse 7, D-91058 Erlangen, Germany

M. Nielsen, M. M. Nielsen, and R. Feidenhans'l
Condensed Matter Physics and Chemistry Department, Risø National Laboratory, DK-4000 Roskilde, Denmark

J. H. Zeysing, O. Bunk, and R. L. Johnson
II. Institut für Experimentalphysik, Universität Hamburg, Luruper Chaussee 149, D-22761 Hamburg, Germany
(Received 9 April 1999)

The surface morphology, composition, and structure of $Au_3Cu(001)$ as determined by scanning tunneling microscopy and surface x-ray diffraction are presented. Atomic resolution STM images reveal distinctive geometric features. The analysis of the surface x-ray diffraction data provides clear evidence of gold enrichment of the topmost layer with two different gold positions and only a small copper fraction. The second layer has approximately Cu_4Au stoichiometry, whereas the third layer is pure gold. STM images and SXRD results are in excellent agreement and reveal a detailed atomic model for the surface structure.
[S0163-1829(99)04535-X]

I. INTRODUCTION

Copper-gold alloys are the standard textbook example of a metallic binary system and have been extensively studied in the past.[1–4] The Cu-Au system is considered to be a classic paradigm for theoretical calculations of phase diagrams and phase stability (Ref. 5, and references therein). Nevertheless, there remain a number of open questions to be answered experimentally concerning the phase stability and chemical ordering in the near-surface region. Gold-copper alloys have a negative mixing enthalpy and form stable phases with the low-temperature Cu_3Au (Ll_2) and CuAu (Ll_0) structures. In the past most attention has been focused on alloys with nominal Cu_3Au composition which exhibits a bulk first-order phase transition. Comparatively little is known about the gold-rich region of the phase diagram. Segregation processes can influence ordering transitions at surfaces and considerably increase their complexity. Surface segregation of gold is frequently observed in gold-containing alloys.[6–8] Recent surface studies on Au_3Cu found the surprising result that oxygen chemisorption enhanced the copper concentration in the top-most layer.[9] We expect gold segregation at Au_3Cu surfaces and concomitant changes in the chemical composition in the near-surface region.[10]

Scanning tunneling microscopy (STM), low energy electron diffraction (LEED), and surface x-ray diffraction (SXRD) are established techniques for determining surface structures. Here, we present data acquired with these techniques on $Au_3Cu(001)$-samples that revealed the composition of the surface layers and the geometrical structure of the surface and near-surface region.

II. EXPERIMENT

The $Au_3Cu(001)$ single crystal was prepared by repeated cycles of ion bombardment with 0.5 keV Ar^+-ions for 30–50 min followed by annealing at 873 K for 2 h at below 5×10^{-10} mbar. Sample temperatures were measured with an infrared pyrometer. The sample was cooled down to the predicted[5] phase-transition temperature of 472 K at 2 K/min and was held at this temperature for 40 h, after which the surface structure was checked by LEED. Figure 1 shows a typical LEED image with a $p(1\times1)$ pattern. The STM images presented here were acquired at room temperature with negative sample bias, using an electrochemically etched tungsten tip. For the SXRD measurements the samples were transferred under UHV in a small portable chamber ($p \leqslant 5 \times 10^{-10}$ mbar) to the vertical diffractometer on the BW2 wiggler beamline at HASYLAB. To avoid fluorescence the SXRD dataset was recorded at an energy of 8.8 keV below

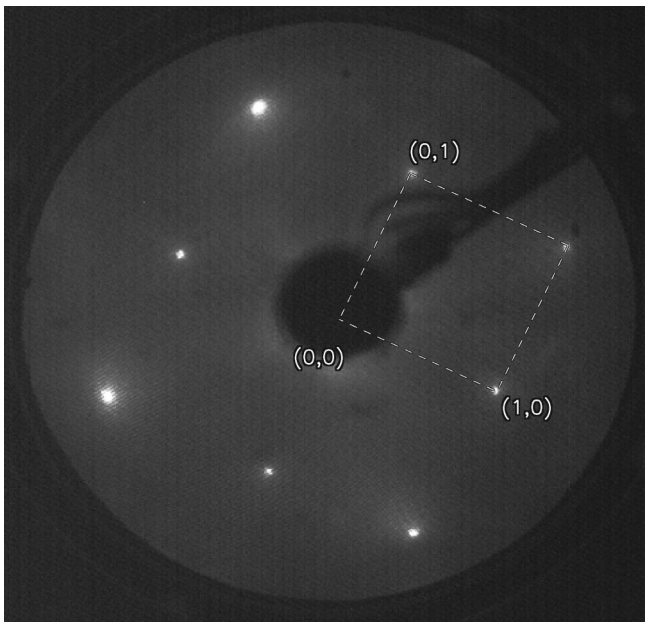

FIG. 1. Typical LEED pattern obtained from the clean and well-annealed $Au_3Cu(001)$ surface (electron energy 120 eV).

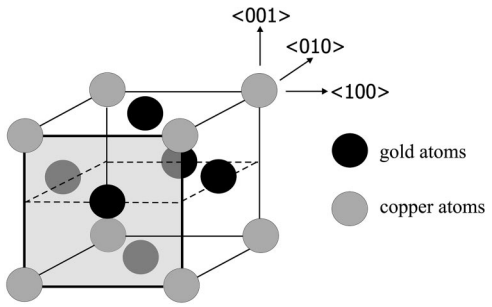

FIG. 2. Crystal structure of the ideal Au_3Cu crystal with $L1_2$ structure.

the Cu-K_α absorption edge. Surface sensitivity was enhanced by using a grazing incidence angle of 0.5°, i.e., close to the critical angle. In total five crystal truncation rods (CTR's) were measured corresponding to 148 reflections. Averaging symmetry-equivalent reflections resulted in a systematic error of 12.5%. Additionally 64 reflections were measured along the specular $(00l)$ rod. In total the dataset consisted of 177 symmetry-inequivalent reflections. In the SXRD data analysis we use LEED coordinates with $\mathbf{a}=1/2[110]_{\text{cubic}}$, $\mathbf{b}=1/2[\bar{1}10]_{\text{cubic}}$, and $\mathbf{c}=[001]_{\text{cubic}}$. The cubic coordinates are given in units of the Au_3Cu lattice constant, therefore $|a|=|b|=2.82$ Å and $|c|=3.99$ Å. The absolute values of the reciprocal coordinates including a factor of 2π are $|a^*|=|b^*|=2.23$ Å^{-1} and $|c^*|=1.57$ Å^{-1}.

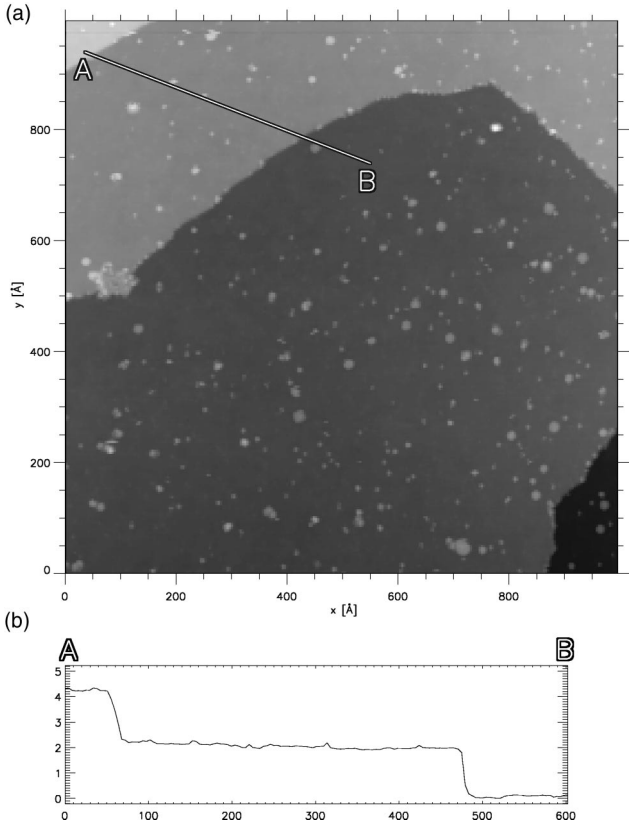

FIG. 3. (a) STM image (1000 Å × 1000 Å) of the topography of $Au_3Cu(001)$ surface. $U_T=-1.350$ mV, $I_T=1.509$ nA. (b) Height profile along $\overline{AB}$.

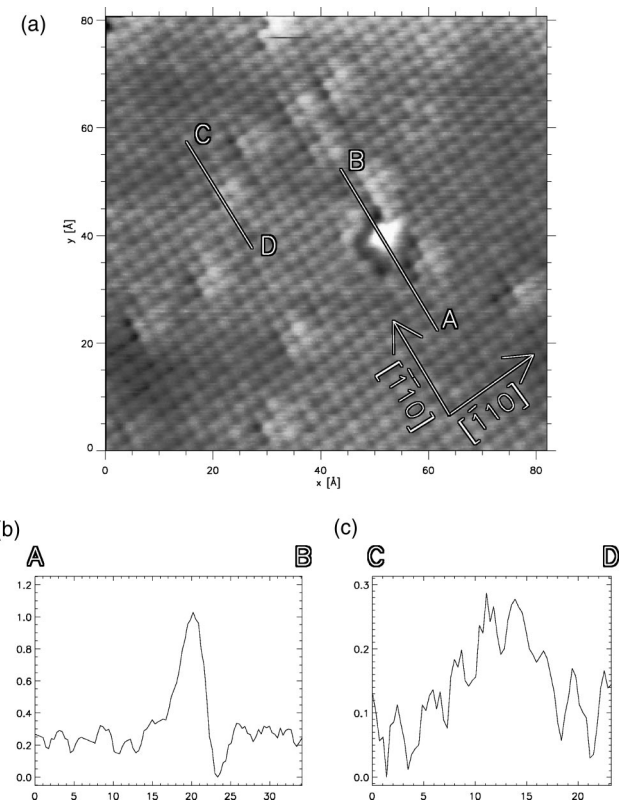

FIG. 4. (a) High resolution STM image (81 Å × 82 Å) of the $Au_3Cu(001)$ surface taken at $U_T=-1.351$ mV, $I_T=1.508$ nA. Two different features are clearly visible. (b) Height profile along $\overline{AB}$ feature (I). (c) Height profile along $\overline{CD}$ feature (II).

III. RESULTS

A. UHV-STM studies

It has been reported that Au_3Cu exhibits an ordered low-temperature phase with the $L1_2$ structure, however, recent density functional calculations indicate that this is not the case and that an ordered (001) superlattice is energetically more favorable.[5] Figure 2 shows the unit cell of an ideal truncated Au_3Cu crystal with $L1_2$ structure. Figure 3 shows an STM image from a $Au_3Cu(001)$ surface with an area 1000 Å × 1000 Å. There are large terraces extending over several hundred Å that are separated by monoatomic steps with a height of 2 Å. The height of the steps corresponds to half of the lattice constant of 3.99 Å determined from the x-ray measurements. Figure 4 shows a higher magnification image in which the atomic 1×1 structure is clearly resolved. The profile along $\overline{AB}$ shows a feature which is located 0.8–1.1 Å above the surface and occupies an area of four by four lattice sites. The shape of this feature varies, but the area occupied is always the same. In the following we will call this feature (I). The profile $\overline{CD}$ goes through a smaller corrugation which lies 0.1–0.2 Å above the surface. There are always four atoms in a (2×2) matrix which are imaged higher than the surrounding atoms (feature (II)). Similar features can be found in Fig. 5. Statistical analysis of the STM images revealed the relative abundances of the different features: $5.7\pm0.5\%$ of the surface consisted of feature (I) and $11.6\pm0.5\%$ of the surface consisted of feature (II).

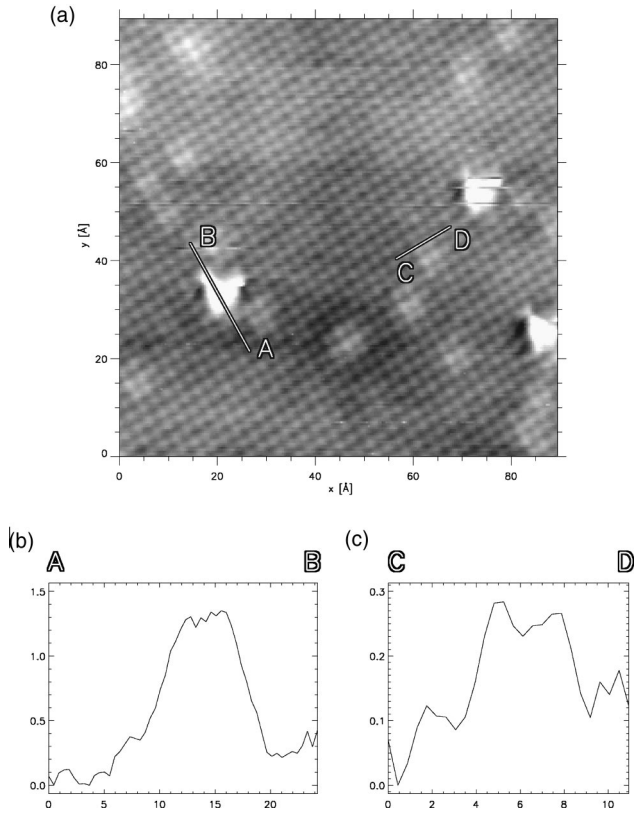

FIG. 5. (a) STM image (90 Å × 90 Å) of the $Au_3Cu(001)$ surface taken at $U_T = -0.992$ mV, $I_T = 1.509$ nA. The two different features are visible. (b) Height profile along $\overline{AB}$ feature (I). (c) Height profile along $\overline{CD}$ feature (II).

B. Surface x-ray diffraction

The $Au_3Cu(001)$ surface exhibits a $p(1\times1)$ periodicity so the structural analysis is based on the crystal truncation rods (CTR's) that contain both surface and bulk information. The specular reflectivity, i.e., the intensity measured along the $(00l)$ rod, only depends on the electron density in the direction perpendicular to the crystal surface, and can be measured to high l values. The information from such reflectivity measurements is particularly useful for eliminating unphysical structural models. In order to reveal the full geometrical structure measurements with in-plane momentum transfer are also necessary.

The absence of reflections specific for the ordered Au_3Cu bulk structure indicates that the bulk crystal was disordered, i.e., the fcc lattice sites are occupied with probabilities of 75% for Au atoms and 25% for Cu atoms.

We started the data analysis with the model proposed by Schömann *et al.*[6] which consists of a Au surface layer and a pure Cu layer beneath it on top of the bulk crystal. Using this model we were unable to fit our data adequately. The theoretical intensity profiles for the crystal truncation and specular rods calculated using this model are shown as dashed lines in Figs. 6 and 7.

In the following structure determination we included several atomic layers and allowed the chemical occupation of the lattice sites in these layers to vary. Because of the $p2mm$ symmetry of the surface only variations of the z position were allowed. Despite some improvement the quality of the fit was still not convincing. For an adequate description of the data we had to include the possibility of a stacking fault in the second layer, i.e., second layer atoms are located directly above third layer atoms. The structure refinement resulted in an excellent reproduction of the experimental data as shown in Figs. 6 and 7 with a reduced χ^2 of 1.9. The parameters we obtained are listed in Table I.

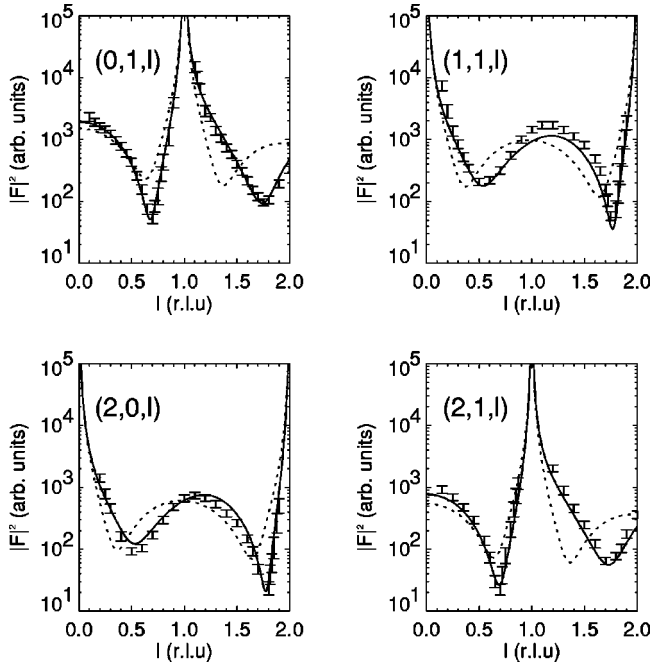

FIG. 6. Crystal truncation rods from the $Au_3Cu(001)$-(1×1) surface. The solid line is calculated using the parameters in Table I. The dashed line is calculated using a model which is described by a topmost gold layer on a copper layer which are on the bulk crystal.

In contrast to the model by Schömann *et al.* the Au concentration in the 3rd layer is 100%. To test the correctness of this model we set the 3rd layer to the bulk stoichiometry of 75% Au and 25% Cu. This resulted in a reduced χ^2 of 9.4. Reoptimizing all parameters lowered the χ^2 value to 3.3 which is still considerably larger than the value of 1.9 for the best set of parameters. Hence the deviation from the bulk Au concentration in the third layer is a significant effect.

In the data analysis only two atomic displacement parameters (ADPS) were used. The value determined for the Au

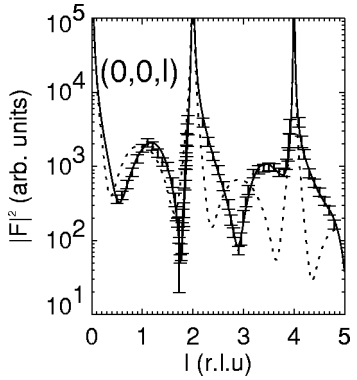

FIG. 7. Specular $(00l)$ rod measured on the $Au_3Cu(001)$-(1×1) surface. The solid line was calculated using the parameters in Table I. The dashed line is calculated using a model which is described by a topmost gold layer on a copper layer which are on the bulk crystal.

TABLE I. Results from the SXRD data analysis. The *fraction* gives the probability that an atom of the *layer* is of the given sort at the given position. The *x*, *y*, and *z* positions are given in the LEED coordinates (see experimental section) and the *z* position is also given in Å. Atomic displacement parameters of 2.2 Å^2 (bulk) and 1.6 Å^2 (Au atoms in top two layers) were found.

layer	atom	fraction [%]	(x, y)-pos. [L]	z-pos. [L]	z- pos. [Å]
1st	Cu	5.3	(0.0,0.0)	1.64	6.58
	Au	10.9	(0.0,0.0)	1.43	5.75
	Au	81.4	(0.0,0.0)	1.40	5.63
2nd	Au	5.8	(0.0,0.0)	1.10	4.43
	Au	11.0	(0.5,0.5)	1.00	4.03
	Cu	79.5	(0.5,0.5)	0.92	3.71
3rd	Au	100.0	(0.0,0.0)	0.50	2.04
4th	Au	75.0	(0.5,0.5)	−0.01	0.00
	Cu	25.0	(0.5,0.5)	−0.01	0.00

atoms in the first and second layer is 1.6 Å^2 and the value for the remaining atoms is 2.2 Å^2, corresponding to amplitudes of 0.14 Å and 0.17 Å, respectively. Using individual ADPS for the surface atoms reveals, that the first layer Cu atom and the second layer Au atom with an abundancy around 5% exhibit a tendency towards larger values for the ADP. This tendency is probably caused by some static disorder and agrees well with the assignment of the defectlike feature (I) with these atoms, as described in the next section. We have not used individual ADPS for each atom in the final data analysis since the χ^2 value did not improve significantly on introducing these extra parameters.

IV. DISCUSSION

The results presented in the previous section reveal a simple (1×1) structure for the $Au_3Cu(001)$ surface. Combining the STM and SXRD results enables us to propose a model that describes the geometrical structure and the chemical composition of this system. The high resolution STM images showed two features at different heights. Our SXRD analysis gave three positions for the atoms in the topmost layer. We define the surface level to be the position of the atom with a Au occupation probability of 81.4%. The other Au position, with an occupation probability of 10.9% is 0.12 Å higher. This corresponds very well with the height of feature (II) (0.1–0.2 Å) which we observed in our STM images. The abundance of this feature was 11.7% which is similar to the 10.9% found in the SXRD analysis. The third atom in the top layer is a Cu atom, located 0.95 Å above the surface plane. This is just the same as the height of feature (I) in the STM images (0.8–1.1 Å). The relative abundance of this feature was found to be 5.7% in the STM images and the SXRD analysis gave 5.3% which is nearly the same.

The structure and composition of the uppermost layer has now been revealed, however, the gold enrichment at the surface must induce changes in the underlying layers. Fortunately, although STM normally only gives information about atoms in the topmost layer, x-ray diffraction probes deeper and yields information about the structure of underlying layers. We found that from the fourth layer downwards all layers possess the bulk crystal structure with the expected 3:1 ratio of Au and Cu. Even if we allowed atomic displacements down to the sixth layer and variation of the occupation probabilities in the fourth layer the quality of the structural refinement did not improve significantly. We found that the third layer entirely consists of gold atoms located on bulk lattice sites. The second layer is made up of 79.5% Cu and 16.8% Au (the missing 3.7% are due to the uncertainties in the occupation numbers). The 79.5% Cu atoms and 11.0% Au atoms are on fcc bulk lattice sites. The Cu atoms are 0.3 Å lower than the Au atoms. The 11.0% occupation number for the Au atoms corresponds to the relative abundance of the slightly elevated Au atoms in the topmost layer feature (II) in the STM images. Hence, we interpret feature (II) to correspond to sites where Au atoms have replaced Cu atoms

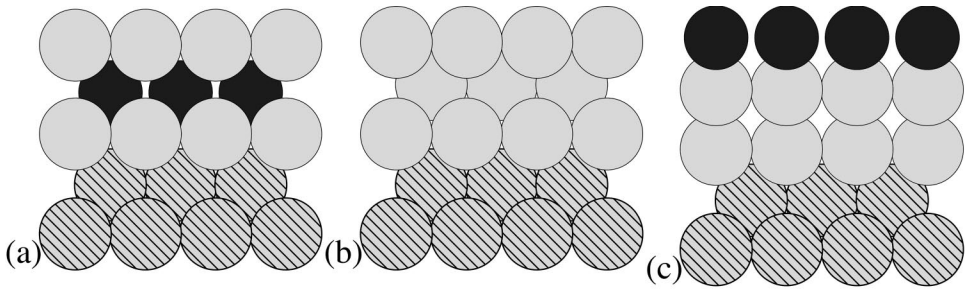

FIG. 8. Proposed models (side view) for the few topmost layers of $Au_3Cu(001)$; Cu atoms are black, Au atoms are gray. Atomic sites with a probability of 75% Au and 25% Cu (bulk structure) are shown as striped circles. (a) 3rd layer: Au (100%), 2nd layer: Cu (79.5%), topmost layer: Au (81.4%) (basic structure); (b) 3rd layer: Au (100%), 2nd layer: Au (11.0%), topmost layer: Au (10.9%) [feature (II)]; (c) 3rd layer: Au (100%), 2nd layer: off-site (on-top) Au (5.8%), topmost layer: Cu (5.3%) [feature (I)].

in the second layer. The rest of the Au atoms in the second layer (5.8%) are located at on-top sites above third layer atoms. This is the reason why the *z* position of these atoms is significantly higher than that of the other atoms in this layer. The value of 5.8% is close to the 5.3 % relative abundance of Cu atoms in the topmost layer. It appears that these Cu atoms are located on top of these ''on-top'' atoms of the second layer. This configuration can be described as a stacking fault—instead of the normal ''*ABAB*'' sequence we have the sequence ''*BAAA*.'' The final structural model is built up from the configurations depicted as side-views in Figs. 8(a)–8(c): (a) corresponds to an ordered superlattice with alternate Au-Cu layers; (b) corresponds to feature (II) from the STM images, and (c) corresponds to feature (I).

V. CONCLUSION

We have investigated in detail the room-temperature phase of $Au_3Cu(001)$ which exhibits a $p(1\times1)$ structure. We have obtained high-resolution STM images which reveal two different features, one at 0.1–0.2 Å and the other at 0.8–1.1 Å above the surface layer. The analysis of our SXRD data led to a model with mixed layers and a stacking fault for a small fraction of atoms in the copper-enriched second layer. The surface layer is composed of gold atoms with a small proportion (5%) of copper atoms and the third layer consists of pure gold. We have assigned the STM features to two different gold and copper atom positions derived from the SXRD analysis. The agreement between the STM and SXRD results and the excellent fit to the structural model (reduced $\chi^2=1.9$) support the correctness of the structure determinated.

ACKNOWLEDGMENTS

Financial support from the DFG under the projects No. STR 295/14-1 and No. DA 436/1-1 and the Graduiertenkolleg ''Physik Nanostrukturierter Festkörper,'' the BMBF under Project No. 05 SB8GUA6, by the TMR-Contract No. ERBFMGECT950059 of the European Community, the Danish Research Council through Dansync and the VW Stiftung is gratefully acknowledged.

*Author to whom correspondance should be adressed: FAX: +49-9131-85-27582.

Electronic address: eckstein@cmp02ww4.ww.uni-erlangen.de

[1] V. S. Sundaram, R. S. Alben, and W. D. Robertson, Surf. Sci. **46**, 653 (1974).

[2] H. C. Potter and J. M. Blakely, J. Vac. Sci. Technol. **12**, 635 (1975).

[3] S. F. Alvarado, M. Campagna, A. Fattah, and W. Uelhoff, Z. Phys. B **66**, 103 (1987).

[4] H. Niehus and C. Achete, Surf. Sci. **289**, 19 (1993).

[5] V. Ozolins, C. Wolverton, and Alex Zunger, Phys. Rev. B **57**, 6427 (1998).

[6] S. Schömann and E. Taglauer, Surf. Rev. Lett. **3**, 1823 (1996).

[7] T. M. Buck, G. H. Wheatley, and L. Marchut, Phys. Rev. Lett. **51**, 43 (1983).

[8] E. G. MacRae, T. M. Buck, R. A. Malic, and W. E. Wallace, Surf. Sci. Lett. **238**, L481 (1990).

[9] S. Nakanishi, K. Kawamoto, N. Fukuoka, and K. Umezawa, Surf. Sci. **261**, 342 (1992).

[10] E. Taglauer, J. du Plessis, and G. N. van Wyk, in *Surface Science Principles and Applications*, edited by R. L. MacDonald, E. Taglauer, and K. Wandelt (Springer, Berlin, 1996), p. 136.